Available online at www.sciencedirect.com

SCIENCE DIRECT®

Magnetic Resonance Imaging 24 (2006) 89–95

MAGNETIC RESONANCE IMAGING

NMR relaxometry and imaging of water absorbed in biodegradable polymer scaffolds

Marta Marcos[a], Pilar Cano[a], Paola Fantazzini[b,*], Carla Garavaglia[b], Santiago Gomez[c], Leoncio Garrido[a]

[a]Department of Physical Chemistry, Institute of Polymer Science and Technology, CSIC, E-28006 Madrid, Spain
[b]Department of Physics, University of Bologna, I-40127 Bologna, Italy
[c]Department of Pathology, Medical School, University of Cádiz, E-11003 Cádiz, Spain

Received 13 September 2005; revised 16 October 2005; accepted 16 October 2005

Abstract

Porous substrates made of poly(3-hydroxybutyrate-3-hydroxyvalerate) (PHBHV) were prepared by a particulate leaching method. After removing the salt by extraction in water, proton nuclear magnetic resonance (NMR) relaxometry and imaging were performed on sets of PHBHV substrates immersed in phosphate-buffered solution during 3 months at different time points. Polarized optical microscopy studies were performed on thin sections, 25 and 5 μm, of the PHBHV samples. The results of NMR relaxometry showed two ^{1}H nuclei populations, well distinguishable on the free induction decay (FID), due to the different decay time constants, a factor of 10^2 apart. Thus, it was possible to separate the two populations, giving separate distributions of T_1 relaxation times. One population could be associated with water protons in the pores and the other to macromolecular protons. The distributions of T_1 and T_2 of the water proton shifted to lower values with increasing immersion time to a constant value after 30 days. The results obtained by NMR imaging showed an initial increase in the apparent porosity, reaching a plateau after 25 days of immersion. This increase is attributed mainly to the absorption of water in the microporosity as supported by the results of the relaxometry measurements and shown by scanning electron microscopy. The average porosity measured by NMR imaging at the plateau, 78±3%, is slightly higher than that determined by optical microscopy, 73±9%, which may be due to the fact that the latter method did not resolve the microporosity. Overall, the results suggest that at early stages after immersing the scaffolds in the aqueous medium, first 30 days approximately, NMR imaging could underestimate the porosity of the substrate.

Keywords: Proton NMR relaxometry; MRI; Scaffold; Biodegradation; Poly(3-hydroxybutyrate-3-hydroxyvalerate)

1. Introduction

Biodegradable synthetic polymers are widely investigated for their application as morphologic guides for tissue regeneration and repair [1,2]. Ideally, a biodegradable substrate should provide initial structural support for cell adhesion and proliferation. It should reabsorb gradually during tissue regeneration and finally be completely absorbed without any detrimental effect to formed tissue. Also, it should allow an efficient mass transport of nutrients and oxygen to a large number of cells in the scaffold. Thus, the design and implementation of these devices require a complete understanding of the aging process, namely, the chemical and structural changes induced in the polymer after implantation and the tissue growth in the scaffold. In general, the degradation of the matrix occurs by the hydrolysis of labile bonds present in the polymer (e.g., C–O in polyesters and polyurethanes, C–N in polyamides and polyurethanes, etc.), leading to a chain breakdown and, ultimately, to the disintegration of the substrate. However, the interaction between implant and tissue is a heterogeneous process. Even in highly porous scaffolds, it has been shown that the degradation of the polymer does not occur homogeneously throughout the whole scaffold [3,4]. Tissue in-growth starts at the periphery of the scaffold and progressively penetrates into it. The development of analytical methods that can sensitively and accurately characterize morphologic changes in bioabsorbable implants will contribute to a better understanding of the degradation mechanisms, cell infiltration and proliferation, and to improving the design of the scaffold.

* Corresponding author. Tel.: +39 51 2095119; fax: +39 51 2090457.
E-mail address: paola.fantazzini@unibo.it (P. Fantazzini).

0730-725X/$ – see front matter © 2006 Elsevier Inc. All rights reserved.
doi:10.1016/j.mri.2005.10.008

The nondestructive and noninvasive nature of the nuclear magnetic resonance (NMR) imaging experiment compared to other techniques available offers a unique opportunity to study in situ time-dependent processes (chemical and morphological) on the same sample. Nuclear magnetic resonance imaging techniques can produce pictures in which the visual contrast (i.e., difference in brightness between separate regions) is related to the observable NMR parameters, which are intrinsic to the sample [5]. Contrast depends on the parameters of the pulse sequence used for the imaging experiment [e.g., flip angle, repetition time (TR), echo time (TE), etc.]. In this case, the observable NMR parameters of interest are the spin-lattice (T_1), homogeneous spin–spin (T_2) and total spin–spin (T_2*) NMR relaxation times of the water protons absorbed in the substrate and the concentration of these protons. Thus, proton density NMR images can map the distribution of water across the sample, and the concentration of water can be correlated with the porosity of the sample or cell density [6,7], but a thorough understanding of the NMR relaxation times of water protons is required.

In this work, the relaxation times of water protons absorbed in scaffolds made of poly(3-hydroxybutyrate-3-hydroxyvalerate) (PHBHV) are studied. These results are correlated with those of morphological studies obtained by using NMR imaging and optical microscopy. Substrates of PHBHV were selected because they are biocompatible and have been used in experimental studies to regenerate structural tissue [8–13]. In addition, previous results have shown that it is possible to map the distribution of water in substrates of PHBHV, both in vitro and in vivo, as a function of implantation time.

2. Materials and methods

2.1. Scaffold preparation

Samples of PHBHV (hydroxybutyrate/hydroxyvalerate: 89:11 mol/mol) (Aldrich, UK) were purified, and their chemical composition was confirmed by analysis with ^{1}H and ^{13}C NMR spectroscopy. Porous matrices were prepared by the particulate leaching method described by Mikos et al. [14] with some modifications. Briefly, the polymers were dissolved in chloroform (10 g/cm^3). The polymer solution was mixed with sodium acetate particles, size ranging from 250 to 350 μm, in a polymer/salt ratio of 20:80 w/w. These choices of particle size and polymer/salt ratio were made considering the requirements estimated for tissue infiltration of a porous substrate. After the solvent was evaporated, samples of polymer/salt composite were immersed in distilled water, changed every 12 h, at 37°C in a shaking water bath to remove the salt until constant weight was reached, between 3 and 5 days. The dry samples were stored in a desiccator under vacuum at room temperature until use.

For the NMR measurements, PHBHV porous substrates were immersed in vials with PBS, and after removing the air trapped within the open pores by vacuum, the vials were placed in a water bath at 25°C and shaken gently. After 24 h, the first series of NMR measurements were acquired according to the protocols described below. After each measurement, the samples were returned to the vials with the buffered solution and placed in the water bath until the next measurement. The procedure was performed many times over 100 days.

2.2. NMR relaxometry

Small samples of polymer scaffolds were immersed in a vial containing PBS, pH=7.4, at 25°C for up to 100 days. At 35 different time points, samples were extracted from the buffer and gently placed in a 10-mm-OD glass tube to be subjected to the relaxation measurements.

Nuclear magnetic resonance relaxometry experiments were performed by a home-built relaxometer based on a JEOL electromagnet, equipped with the NMR console SPINMASTER (Stelar, Pavia, Italy) at 25°C and 20 MHz. To analyze T_1 relaxation times, ^{1}H longitudinal relaxation curves were obtained through inversion-recovery [15] pulse sequences (π-t-π/2-acquisition). The ^{1}H magnetization was acquired with a suitable choice of 64 t values equally spaced in log time and extending from 5 ms to 8 s, to cover all the recovery processes. At each of 64 times, 128 points on the free induction decay (FID) were recorded, with points at 1-μs intervals starting at 14 μs after the end of the π/2 pulse. To analyze T_2 relaxation times, ^{1}H transverse relaxation curves were obtained through Carr–Purcell–Meiboom–Gill (CPMG) [15] pulse sequences with TE (600 μs) under the same temperature and frequency conditions. Quasi-continuous distributions of relaxation times were computed by uniform-penalty inversion (UPEN) [16]. In order to represent the wide relaxation time distributions by means of a compact parameter, experimental relaxation curves were fit to the stretched exponential functions:

$$M(t) = M(\infty)\left[1 - k\,\exp\left(-(t/T_{1s})^{\alpha 1}\right)\right] \quad (1)$$

$$M(t) = M(0)\left[\exp\left(-(t/T_{2s})^{\alpha 2}\right)\right] \quad (2)$$

in order to compute T_{1s} and T_{2s}, the time constants for longitudinal and transverse relaxation, respectively; where $M(t)$ is the acquired signal, $M(0)$ and $M(\infty)$ are the extrapolated values at $t=0$ and $t=\infty$, respectively, and k, $\alpha 1$ and $\alpha 2$ are constants.

2.3. NMR imaging

For imaging, seven PHBHV porous substrates (dimensions ~10×4×2 mm^3) were immersed in vials containing 20 ml of PBS, pH=7.4, at 25°C. After 24 h from the preparation, the first series of NMR images of these samples were acquired by placing them in a 22-mm-OD glass tube inside a 25-mm ∅ radiofrequency coil insert. Once the NMR imaging study was completed, the samples were

returned to the vials with the buffered solution and placed in the water bath until the next NMR measurement. The procedure was performed a total of 15 times over 106 days.

The NMR imaging experiments were performed on a Bruker Avance 400 spectrometer (Bruker BioSpin, Rheinstetten, Germany), equipped with a wide bore, 89-mm ∅, superconducting magnet operating at 9.4 T (proton frequency at 400.13 MHz) and a microimaging accessory. The images were obtained at 25°C using a 2D multislice sequence with a TE of 6.4 ms and a TR of 5 s. Additionally, a set of images with TE of 20, 40, 80 and 160 ms were acquired at Days 11, 32 and 61, after immersion in PBS to determine the effect of TE on the signal intensity measured. Ten slices with a thickness of 500 μm and a field of view of 25×25 mm^2, in-plane resolution of 256 by 256 pixels, were acquired.

The NMR images were processed using NIH Image (NIH, Bethesda, MD) and Bruker Paravision software by two observers independently (PC and LG). In each slice, ROIs were selected and the mean signal intensity measured for each sample, background and medium. The apparent open porosity (i.e., open volume within the sample connected to the outside) for each sample in a given plane was calculated according to the following expression:

$$P_i\ (\%) = 100(S_{si} - S_b)/(S_m - S_b) \qquad (i = 1,..., 7) \qquad (3)$$

where P_i represents the apparent open porosity, expressed in %; S_{si}, S_b and S_m are the mean signal intensities measured in ROIs defined within each sample section, background and medium, respectively. The apparent open porosity for each sample was calculated as

$$P = (1/n)\sum_{j=1}^{n} P_j \qquad (j = 1,..., 10) \qquad (4)$$

In those cases were images were acquired at several TEs, the average signal intensity for the sample and medium at TE=0 was determined by fitting the NMR data to a bi- and monoexponential functions, respectively, and the apparent porosity calculated according to the equations described above.

2.4. Optical microscopy

PHBHV samples were examined first with an SM1500 NIKON stereoscopic microscope, and then PHBHV samples were embedded in glycol-methacrylate and cut as 25- and 5-μm-thick sections using an HM360 MICROM microtome. The optical microscopy was carried out on an Optiphot-2 NIKON microscope using a Coolpix 4500 NIKON digital camera to take the images. The sections were observed under polarized light at magnifications ranging from 4 to 40 times. Five samples were analyzed, and a total of 82 and 100 fields were examined for 25- and 5-μm-thick slices, respectively. The images were processed using NIH Image. To determine the porosity of the samples analyzed, images were converted to grayscale (0–255 levels); a threshold was applied to each image, and pixels with levels ≥72 were assigned to the polymer (pore walls) and the rest to the pores.

2.5. Scanning electron microscopy

Scanning electron microscopy of gold-coated samples was performed on a microscope Philips XL30 (Philips, Eindhoven, NL) at ambient temperature to observe the microarchitecture of the substrates.

3. Results

3.1. NMR relaxometry

Relaxation measurements were performed starting from 24 h after the preparation and repeated 34 times over 96 days. In each sample, the acquired FID appeared to be the sum of an approximately "solid-like" Gaussian component (GC) proportional to $\exp[-\frac{1}{2}(T/T_G)^2]$, where T is time after the end of the π/2 radiofrequency pulse, and T_G is the Gaussian time constant, of the order of 10 μs, and a longer "liquid-like" exponential component (LLC). It is long

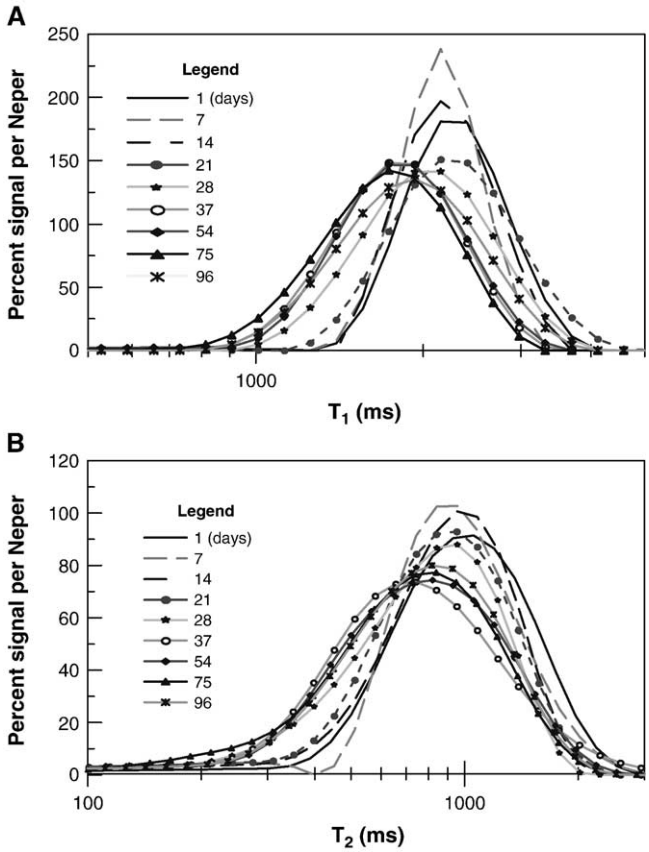

Fig. 1. Choices of relaxation time distribution functions of T_1 (A) and T_2 (B) of water ^1H nuclei obtained by UPEN [16] as a function of time for PHBHV porous substrates in PBS. The ordinate is $dM'/d\ln T_1$, where M' is percent of total signal, in such a way that areas under the curves are normalized to unit area. The shapes of the distribution functions suggest wide distributions of pore sizes. The shift of the distributions suggests the progressive ingress of water in smaller pores during the first 30 days.

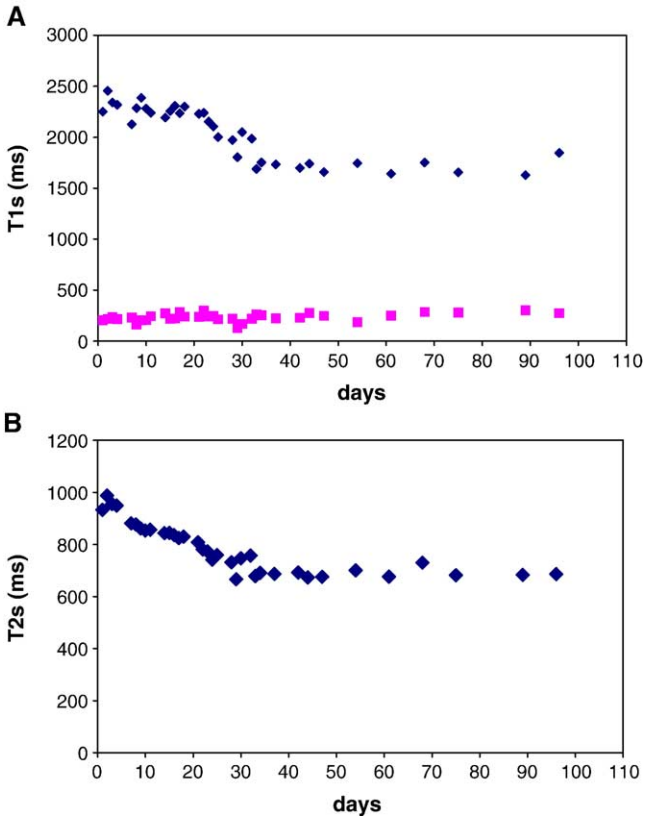

Fig. 2. Compact T_{1s} relaxation time computed for the water and for the macromolecular ^{1}H nuclei (A), and T_{2s} for the water ^{1}H nuclei (B) as a function of immersion time in PBS. While no changes were observed for macromolecular protons, a decrease was observed for both T_{1s} and T_{2s} of the water protons in the first 30 days, still suggesting a progressive increase in that period of time of the surface-to-volume ratio of the pore space invaded by water.

known that such GC component can contribute to the FID in biological tissues and has been ascribed to macromolecular ^{1}H of restricted mobility [17,18], whereas the LLC component is due to water. It has been possible to separate GC from LLC in a reasonably stable and reproducible manner, giving separate T_1 distributions. At the TE used in the CPMG sequence, only the signal from the LLC was acquired. Neither the longitudinal (T_1) nor the transverse (T_2) relaxation curves of LLC were single exponential, and both were analyzed by assuming a quasi-continuous distribution of relaxation times. Fig. 1 shows a choice of T_1 (Fig. 1A) and T_2 (Fig. 1B) distribution functions, in the time course from 1 to 96 days. A clear shift appears from larger to shorter times. The trend is better visualized by plotting the compact stretched exponential times. Fig. 2 shows the plots of T_{1s} for LLC and GC (Fig. 2A) and T_{2s} for LLC (Fig. 2B). While no changes are detectable for T_{1s} of GC, both T_{1s} and T_{2s} of the LLC show a significant decrease during the first 30 days.

3.2. NMR imaging

Seven PHBHV porous substrates immersed in PBS were used. The first images of the seven samples were obtained after 24 h from preparation, and the procedure was repeated 15 times over 106 days, according to the protocol described previously. One example of the NMR images obtained is shown in Fig. 3. The figure illustrates one image plane across the seven samples studied. The signal intensity at each location is proportional to the concentration of water protons. Thus, assuming that the signal intensity in the medium represents 100% porosity, the apparent open porosity of the sample is calculated by Eq. (3). Fig. 4 shows the variation of the apparent open porosity at different times of immersion, from about 55% to a constant value of 78±3%.

In addition, the variation of the signal intensity measured as a function of TE at three time points within the 3-month interval was evaluated. The changes in signal intensity in the medium were best fitted to a monoexponential function, while for the absorbed water protons, the best fit was to a biexponential function. The results showed that the porosity measured by extrapolation of the imaging data to TE=0 ms was about 13% higher than that measured at TE of 6.5 ms. Thus, the values of the open porosity shown in Fig. 4 should be corrected by a factor of 1.13, giving an average open porosity of 88% after the initial 30 days.

3.3. Optical microscopy

A total of five samples were analyzed by optical microscopy. Three samples were examined before immersion in PBS and the other two were analyzed after 106 days

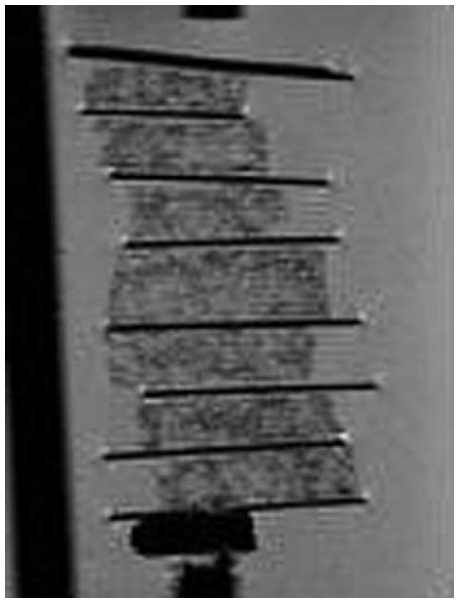

Fig. 3. Proton NMR image showing a section of seven PHBHV porous substrates spaced from each other by glass cover slips (dark lines). The images were acquired using a 2D spin echo multislice sequence with TR of 5 s and TE of 6.4 ms. The slice thickness is 500 μm, and the in-plane resolution is 256 by 256 pixels of 98 by 98 μm^2. The NMR signal intensity is proportional to the concentration of water protons at each pixel, and after normalizing to that of the medium it represents the open porosity (pores interconnected to the outside) of the sample.

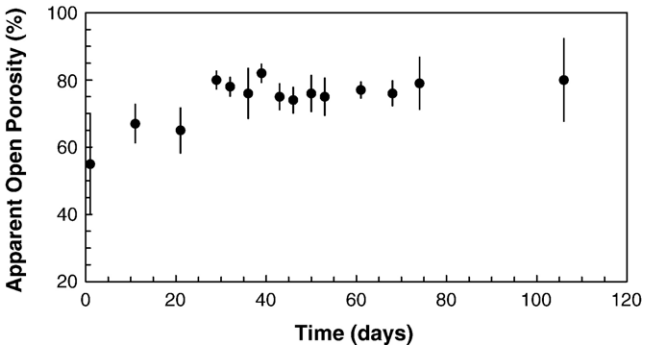

Fig. 4. Variation of apparent open porosity measured by NMR imaging as a function of time in PBS. During the first days of immersion in the aqueous solution, an increase in the mean value of the apparent porosity was observed. Then, after 30 days, it remained unchanged until the end of the experiment.

of immersion in PBS, and the NMR imaging study was completed.

In all cases, PHBHV samples on gross visual examination with the aid of a stereoscopic microscope exhibited a homogeneous view with large open pores. On several of these views, it was estimated that the area associated with these pores represented about 40% of the total outer surface.

Fig. 5(1) illustrates a 4× lens view under polarized light of a 25-μm-thick section corresponding to a PHBHV sample. The bright areas are associated with pore walls normal to the section plane, while the dark areas correspond

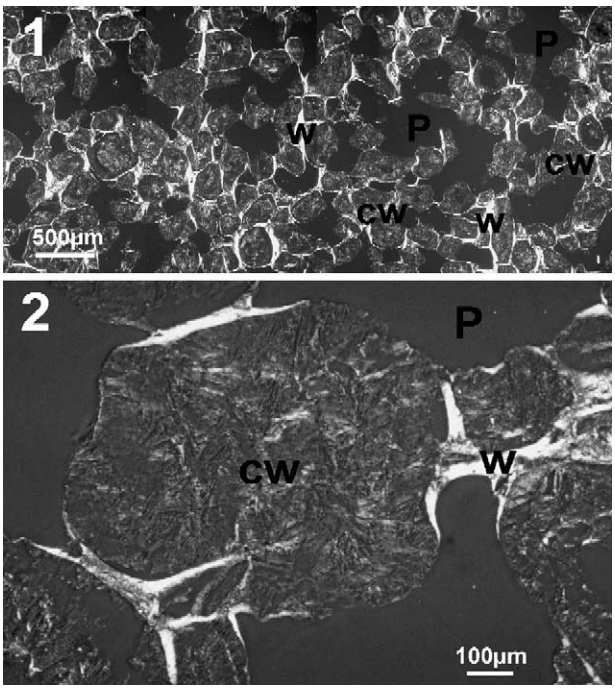

Fig. 5. Optical images corresponding to a (1) 4× lens view of a 25-μm-thick section and a (2) 20× lens view of a 5-μm-thick section of a PHBHV porous substrate. The black (P) and bright (W) areas correspond to the pores and pore walls normal to the cross-section plane, respectively. The gray (CW) areas are associated with the pore walls contained within the section plane.

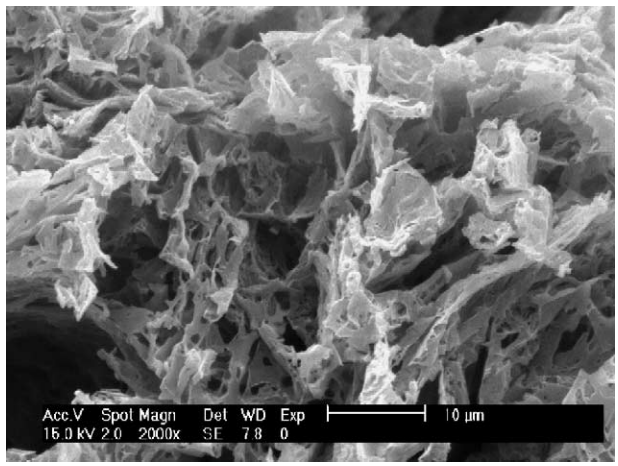

Fig. 6. Scanning electron micrograph of a cross section of a PHBHV sample. In addition to large pores, the presence of micropores was observed.

to interconnecting pores with adjacent planes. The gray areas represent the pore walls contained within the section. This is visualized more clearly in Fig. 5(2) where a 20× lens view of a 5-μm-thick section is shown. The measurements of areas assigned to polymer or empty space in binary images corresponding to 80 fields of the 25-μm-thick sections and 100 fields of the 5-μm-thick sections combined gave a mean value of porosity equal to 73% (S.D.=9). This result represents a measure of the macroporosity of the sample, and it is in fair agreement with the value of apparent porosity calculated from NMR imaging measurements.

3.4. Scanning electron microscopy

Fig. 6 shows a scanning electron micrograph corresponding to a cross section of a PHBHV porous substrate. In addition to large pores, the presence of very small pores could be observed, which could have been formed by the evaporation of the solvent during the preparation of the scaffold.

4. Discussion

Nuclear magnetic resonance imaging has been proposed as a noninvasive technique to monitor cell proliferation and tissue infiltration in biodegradable scaffolds [7,19,20]. This is based on the fact that the behavior of T_1 and T_2 relaxation times of protons associated with free water is longer than that of water present in cellular cytoplasm. Thus, for a given set of NMR imaging parameters, it is expected to observe a change in signal intensity within the scaffold that could be correlated to the proliferation of cells after seeding in vitro or to tissue infiltration after implantation in vivo. However, changes observed in the relaxation times of water might not be entirely due to the presence of cells when scaffolds are made of biodegradable polymers since, in these cases, an interaction between polymer and aqueous media (i.e., swelling of the polymer matrix, chain scission) may occur.

Nuclear magnetic resonance imaging allowed the mapping of the apparent open porosity of the substrates over the period of time studied. The results showed an initial increase in the apparent porosity, reaching a plateau after 25 days of immersion. This could be due in part to the shortening of the relaxation time of water, since the TR used in the imaging experiment leads to partial saturation of the NMR signal, particularly at the initial stages of sample immersion in the aqueous medium. In addition, the absorption of water in the microporosity of the polymer matrix as supported by the results of the relaxometry measurements will contribute to increasing the apparent value of porosity. This might be a slow process due to the lipophilic character of the PHBHV [21].

The results of NMR relaxometry showed two ^{1}H nuclei populations, well distinguishable on the FID. It was possible to separate the two populations on the basis of the very different FID time constants (a factor 100 apart), giving separate distributions of T_1 relaxation times. One population could be associated with water protons in the pores with T_1 of the order of 2 s and the other to macromolecular protons with T_1 of the order of 250 ms. While the relaxation times of the macromolecular protons did not change, the distributions of T_1 and T_2 of the water protons shifted to lower values with immersion time to a constant value after 30 days. The decrease of these relaxation times, the relaxation of the macromolecular protons being unchanged, strongly suggests that the open porosity was increasing during the first 30 days by the addition of microporosity, with high surface-to-volume ratios, where the water relaxation time is shorter. Indeed, the microporosity in the PHBHV samples was observed by scanning electron microscopy analysis.

After an initial period of about a month, the porosity measured by NMR imaging at the plateau is in fair agreement with that determined by optical microscopy.

5. Conclusions

The NMR relaxometry and imaging results suggest at early stages after immersing the matrix in the aqueous medium water filling the microporosity of the sample. For PHBHV scaffolds during this period, 30 days approximately, NMR imaging could underestimate the open porosity of the substrate. Therefore, it is suggested to take into consideration these results when using NMR imaging to map changes in water proton relaxation times in scaffolds and make use of those changes to evaluate degradation and cell infiltration and proliferation in biodegradable polymer substrates, both in vitro and in vivo.

Acknowledgments

The authors acknowledge the financial support provided by the Spanish Ministry of Health, “Fondo de Investigación Sanitario,” FIS 01/1070, and by the CICYT, MAT 2001/2130 (M.M., P.C., L.G.), University of Bologna, and MIUR FIRB-2001 (P.F., C.G.), and RED G03-122 of Institute Carlos III (S.G.), and by ESA ESTEC 16824/02/NL/VJ.

References

[1] Langer R. Polymers for drug delivery and tissue engineering. Ann Biomed Eng 1995;23:101–11.
[2] Langer R, Tirrell DA. Designing materials for biology and medicine. Nature 2004;428:487–92.
[3] Lu L, Garcia CA, Mikos AG. In vitro degradation of thin poly (DL-lactic-co-glycolic acid) films. J Biomed Mater Res 1999;46:236–44.
[4] Lu L, Peter SJ, Lyman MD, Lai H-L, Leite SM, Tamada JA, et al. In vitro and in vivo degradation of porous poly (DL-lactide-co-glycolic acid) foams. Biomaterials 2000;21:1837–45.
[5] Mansfield P, Morris PG. Advances in magnetic resonance. Suppl 2. NMR imaging in biomedicine. New York: Academic Press; 1982.
[6] Garrido L. Nondestructive evaluation of biodegradable porous matrices for tissue engineering. In: Morgan JR, Yarmush ML, editors. Tissue engineering methods and protocols. Methods in Molecular Medicine, vol. 18. Totowa (NJ): Human Press Inc; 1999. p. 35–45.
[7] Garrido L. Non-destructive evaluation of synthetic tissue scaffolds with NMR. Mater Res Soc Proc (Materials Research Society) 1999;550:171–6.
[8] Knowles JC, Hastings GW, Ohta H, Niwa S, Boerre N. Development of a degradable composite for orthopaedic use: in vivo biomechanical and histological evaluation of two bioactive degradable composites based on the polyhydroxybutyrate polymer. Biomaterials 1992;13:491–6.
[9] Gogolewski S, Jovanovic M, Perren SM, Dillon JG, Hughes MK. Tissue response and in vivo degradation of selected polyhydroxyacids: polylactides (PLA), poly(3-hydroxybutyrate) (PHB), and poly(3-hydroxybutyrate-co-3-hydroxyvalerate) (PHB/VA). J Biomed Mater Res 1993;27:1135–48.
[10] Deng Y, Zhao K, Zhang Xf, Hu P, Chen GQ. Study on the three-dimensional proliferation of rabbit articular cartilage-derived chondrocytes on polyhydroxyalkanoate scaffolds. Biomaterials 2002;23:4049–56.
[11] Köse GT, Kenar H, Hasirci N, Hasirci V. Macroporous poly (3-hydroxybutyrate-co-3-hydroxyvalerate) matrices for bone tissue engineering. Biomaterials 2003;24:1949–58.
[12] Köse GT, Korkusuz F, Korkusuz P, Purali N, Özkul A, Hasirci V. Bone generation on PHBV matrices: an in vitro study. Biomaterials 2003;24:4999–5007.
[13] Köse GT, Korkusuz F, Özkul A, Soyal Y, Özdemir T, Yildiz C, et al. Tissue engineered cartilage on collagen and PHBV matrices. Biomaterials 2005;26:5187–97.
[14] Mikos AG, Thorsen AJ, Czerwonka LA, Bao Y, Langer R, Winslow DN, Vacanti JP. Preparation and characterization of poly(L-lactic acid) foams. Polymer 1994;35:1068–77.
[15] Callaghan PT. Principles of nuclear magnetic resonance microscopy. Oxford: Clarendon Press; 1991.
[16] Borgia GC, Brown RJS, Fantazzini P. Uniform-penalty inversion of multiexponential decay data II: Data spacing, T_2 data, systematic data errors, and diagnostics. J Magn Reson 2000;147:273–85 [ibid. 1998;132:65–77].
[17] Edzes HT, Samulski ET. The measurement of cross-relaxation effects in the proton NMR spin-lattice relaxation of water in biological systems: hydrated collagen and muscle. J Magn Reson 1978;31:207–29.
[18] Fantazzini P, Bortolotti V, Brown RJS, Camaiti M, Garavaglia C, Viola R, Giavaresi G. Two ^{1}H-NMR methods to measure internal

porosity of bone trabeculae: by solid–liquid signal separation and by longitudinal relaxation. J Appl Phys 2004;95:339–43.

[19] Hartman EH, Pikkemaat JA, Van-Asten JJ, Vehof JW, Heerschap A, Oyen WJ, et al. Demineralized bone matrix-induced ectopic bone formation in rats: in vivo study with follow-up by magnetic resonance imaging, magnetic resonance angiography, and dual-energy X-ray absorptiometry. Tissue Eng 2004;10:747–54.

[20] Watrin-Pinzano A, Ruaud JP, Cheli Y, Gonord P, Grossin L, Bettembourg-Brault I, et al. Evaluation of cartilage repair tissue after biomaterial implantation in rat patella by using T2 mapping. Magma 2004;17:219–28.

[21] Hasirci V, Tezcaner A, Hasirci N, Süzer S. Oxygen plasma modification of poly(3-hydroxybutyrate-co-3-hydroxyvalerate) film surfaces for tissue engineering purposes. J Appl Polym Sci 2003;87:1285–9.